The Use of DFDR Information in the Analysis of a Turbulence Incident over Greenland

PETER F. LESTER AND ORHAN SEN*

Department of Meteorology, San Jose State University, San Jose, California

R. E. BACH, JR.

NASA-Ames Research Center, Moffett Field, California

14 July 1988 and 1 December 1988

ABSTRACT

Digital flight data recorder (DFDR) tapes from commercial aircraft can provide useful information about the mesoscale environment of severe turbulence incidents. Air motion computations from these data and their errors are briefly described. An example of mesoscale meteorological information available from DFDR tapes is presented for a case of turbulence in mountain waves over the Greenland icecap.

1. Introduction

The study of Clear Air Turbulence (CAT) depends primarily on the collection of data with aircraft. While some excellent comprehensive studies have been accomplished with specially instrumented aircraft (e.g., Dutton 1969; Lilly 1978), CAT forecast development and verification studies have depended mainly on commercial aircraft. The latter data collection efforts are complicated by the semiquantitative nature of most CAT reports and the tendency for aircraft to stay away from areas where severe CAT has been predicted or observed. The result is that CAT forecast studies must deal with the correlation of relatively few reports of marginal quality with synoptic patterns (Colson 1963), radiosonde data (Endlich and Mancuso 1965; Keller 1986), and satellite patterns (Ellrod 1985).

In the last few years, a new dimension has been added to the study of turbulence in the free atmosphere. Most wide-bodied commercial aircraft now carry digital flight data recorders (DFDR); careful analysis of that information not only allows the quantification of turbulence events, but gives unprecedented information on the mesoscale environment of the turbulence. Lilly and Petersen (1983), Nastrom and Gage (1983) and Gysel and Richner (1986) have discussed the usefulness of such data as collected in special programs.

Under normal operations, data tapes are retained for later analysis only when the aircraft are involved in unusual events such as extreme turbulence. Scientists at NASA-Ames Research Center have obtained several sets of such data and have performed analyses to better understand the nature of the turbulence and its effects on aircraft (e.g., Parks et al. 1985, Lester and Bach 1986). The purpose of this note is to give a brief description of computational procedures for air motions and to illustrate the potential utility of the DFDR data with a documentation of a turbulence incident over Greenland.

2. Wind estimation from DFDR data

The measurement set available from a digital flight recorder, along with (ATC) radar data and aircraft performance information, is used in a postflight analysis to estimate winds encountered along the flight path. A block diagram of the procedure is shown in Fig. 1. The method for wind extraction, based on rigid-body kinematics (Bach and Wingrove 1989), is outlined below.

The analysis begins by expressing vehicle accelerations in the earth frame (here considered to be locally flat, with the x-axis pointing north, the y-axis east, and the h-axis vertical) as

$$\begin{aligned}\ddot{x} &= a_x \cos\Theta \cos\psi + a_y(\sin\phi \sin\Theta \cos\psi - \cos\phi \sin\psi) \\ &\quad + a_z(\cos\phi \sin\Theta \cos\psi + \sin\phi \sin\psi) \\ \ddot{y} &= a_x \cos\Theta \sin\psi + a_y(\sin\phi \sin\Theta \sin\psi + \cos\phi \cos\psi) \\ &\quad + a_z(\cos\phi \sin\Theta \sin\psi - \sin\phi \cos\psi) \\ \ddot{h} &= a_x \sin\Theta - (a_y \sin\phi + a_z \cos\phi) \cos\Theta - g, \end{aligned} \tag{1}$$

where (a_x, a_y, a_z) are onboard measurements of body-axis accelerations and (ϕ, Θ, ψ) are onboard measurements of body-axis Euler angles. Integration of the dif-

* Visiting professor, Istanbul Technical University.

Corresponding author address: Dr. Peter F. Lester, Dept. of Meteorology, San Jose State University, San Jose, CA 95192-0104.

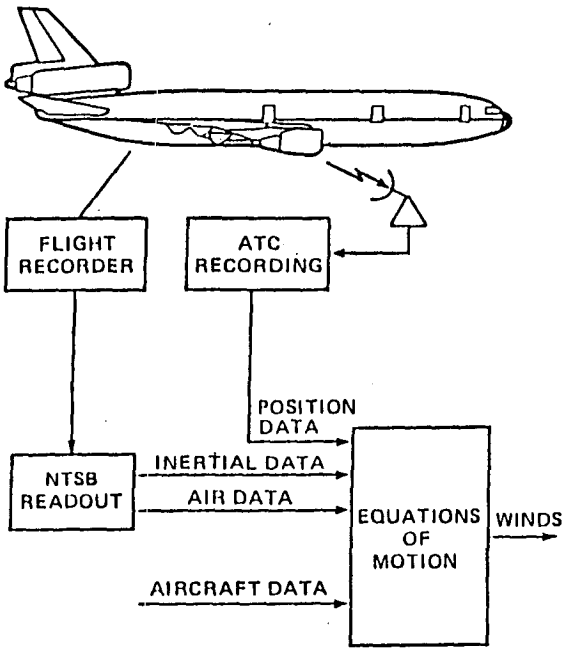

FIG. 1. Estimation of winds from airline operating records. "ATC recording" refers to Air Traffic Control radar position data. "NTSB Readout" is that portion of the DFDR (flight recorder) tape made available from the National Transportation Safety Board to NASA-Ames. "Air data" include temperature, airspeed, angle of attack and sideslip angle.

ferential equations provides estimates of inertial velocity ($\dot{x}$, $\dot{y}$, $\dot{h}$) and position (x, y, h). A set of initial conditions and bias corrections are determined by matching the calculated x and y time-histories to radar position data and the h time-history to the measured altitude.

The wind velocity is now computed as the difference between the vehicle inertial velocity and its velocity with respect to the air mass. The wind components in the earth frame are given by

$$w_x = \dot{x} - V\cos\Theta_w \cos\psi_w$$
$$w_y = \dot{y} - V\cos\Theta_w \sin\psi_w$$
$$w_h = \dot{h} - V\sin\Theta_w, \qquad (2)$$

where true airspeed V is computed from the flight records and where wind-axis Euler angles (Θ_w, ψ_w) are found using the identities

$$\sin\Theta_w = \cos\alpha\cos\beta\sin\Theta - C\cos\Theta$$
$$\tan(\psi_w - \psi) = \frac{\sin\beta\cos\phi - \sin\alpha\cos\beta\sin\phi}{\cos\alpha\cos\beta\cos\Theta + C\sin\Theta},$$

where

$$C = \sin\alpha\cos\beta\cos\phi + \sin\beta\sin\phi. \qquad (3)$$

In Eq. (3), α is the angle of attack and β is the sideslip angle.

The DFDR flight records often include a vane-angle measurement from which the angle of attack may be derived. When no vane measurement exists, angle of attack may be estimated from the equation

$$C_L = C_L(\alpha, \delta_F) + C_{L_{\delta_e}}\delta_e + C_{L_q}(\bar{c}q/2V), \qquad (4)$$

where $C_L(\alpha, \delta_F)$, $C_{L_{\delta_e}}$, and C_{L_q} are based on the aircraft aerodynamics and $\bar{c}$ is the mean wing chord. The lift coefficient C_L, flap position δ_F, elevator position δ_e, and pitch rate q are derived from the flight recorder data, leaving the angle of attack α as the solved variable (Bach and Parks 1987). In a similar manner the sideslip angle may be estimated from the equation

$$C_Y = C_{Y_\beta}\beta + C_{Y_{\delta_r}}\delta_r + C_{Y_r}(br/2V), \qquad (5)$$

where C_{Y_β}, $C_{Y_{\delta_r}}$, and C_{Y_r} are based on the aircraft aerodynamics and b is the wing span. The side-force coefficient C_Y, rudder position δ_r, and yaw rate r are derived from the flight recorder data, leaving the sideslip angle β as the solved variable (Bach and Parks 1987).

Lenschow (1986) gives expressions equivalent to Eqs. (1)–(3) for the determination of air motions from instrumented aircraft from the National Center for Atmospheric Research (NCAR). In contrast to airline DFDR systems, the NCAR aircraft measurement systems are designed especially for turbulence measurements and include accurate pressure, flow, and temperature sensing devices to provide the air data (α, β, V), as well as an inertial navigation system (INS) to provide (a_x, a_y, a_z) and (ϕ, Θ, ψ) for evaluation of the wind components. Clearly, the limited measurement capabilities of the commercial aircraft will result in significantly larger errors in wind and vertical velocity determinations.

Estimates of the errors involved in the air motion calculations can be made if the uncertainties in measurements are assumed to be statistically independent and α, β, ϕ and Θ are small. Under these conditions, the error in the horizontal velocity component is given by

$$\delta w_{xy} \approx [\delta^2 V_{xy} + \delta^2 V + V^2\delta^2(\psi + \beta)]^{1/2}, \qquad (8)$$

where δV_{xy} is the error in the horizontal-plane component of inertial velocity. Similarly, the error in the vertical velocity component is given by

$$\delta w_h \approx [\delta^2\dot{h} + V^2\delta^2(\Theta - \alpha)]^{1/2}. \qquad (9)$$

Table 1 shows typical rms errors for horizontal and vertical velocity components for the airliner encounters analyzed at Ames Research Center. Note that the errors in Table 1 are 40%–50% greater than those estimated for NCAR aircraft (Lenschow 1986).

3. The Greenland incident

At 1654 UTC 22 January 1985, Pan American Flight 125 (B-747) was westbound over southern

TABLE 1. Rms errors (DFDR plus radar track).

Level flight, $V = 250$ m s^{-1}

δw_{xy}		δw_h	
Error source	Error (m s^{-1})	Error source	Error (m s^{-1})
δV_{xy}	1.0	$\delta \dot{h}$	1.0
δV	1.0	$V\delta(\Theta - \alpha)$	2.0
$V\delta(\psi + \beta)$	2.0		

Greenland at 33 000 feet (10 km) MSL when it encountered a series of increasingly violent vertical oscillations over a period of a few minutes. The turbulence culminated in a sudden altitude gain of 1000 feet (300 m). Vertical accelerations reached $+2.7g$, $-1.0g$, and injuries were sustained by several passengers and crew. The location of the incident is shown in Fig. 2 at 62°N, 48°W.

A previous analysis of this incident was performed by Forrester (1986) using conventional PIREPS and meteorological analyses. He concluded that the turbulence was most likely due to flight through the delta region of a bifurcated jet stream over southern Greenland. The jet stream feature was on the eastern periphery of a strong cyclone located southwest of Greenland. From 1200 UTC 22 January until 0000 UTC 23 January (Fig. 2), winds over the southern portion of the ice cap gradually shifted from southwesterly to southeasterly and speeds increased significantly. About seven hours after the incident, the delta region is apparent at the ridge line east of Greenland in Fig. 2.

Further large scale analyses by the authors included the construction of vertical cross sections and long sections through the site of the turbulence. In general, the

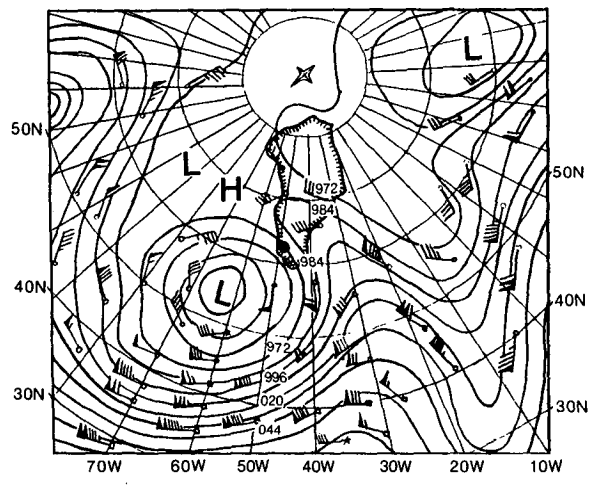

FIG. 2. 250 mb analysis for 0000 UTC, 23 January 1985 redrawn for clarity from NMC analysis with plotted rawinsonde, aircraft and satellite wind data (knots). Contours drawn at 120 dam intervals. The site of turbulence incident which occurred about 7 h prior to map time is indicated with a black dot.

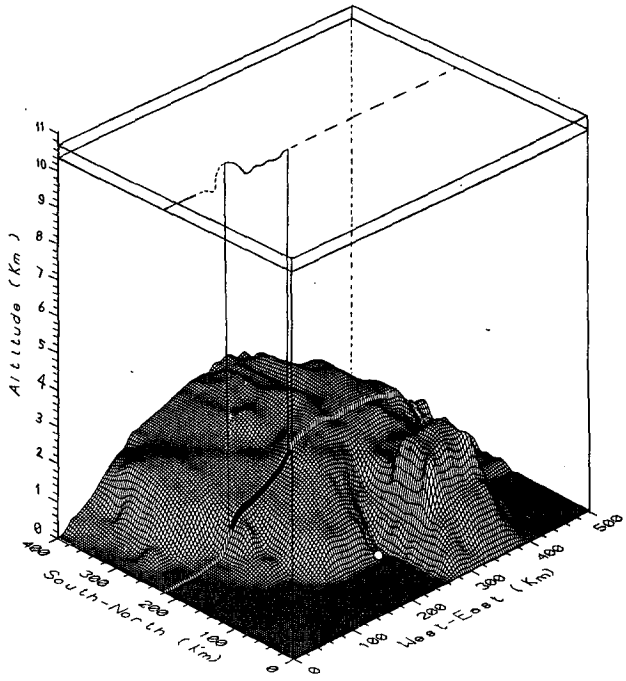

FIG. 3. Perspective diagram of southern Greenland (smoothed terrain). Aircraft track is shown at altitude and projected onto the surface. Track segment for which DFDR data were analyzed is shown as a thin solid line aloft, and a thick solid line on the surface. Elsewhere, the aircraft track configuration was estimated from the pilot's log. The location of Narssarssuaq is shown by the white dot.

results (not shown) were in agreement with Forrester (1986), i.e., the turbulence incident occurred on the anticyclonic side of the jet core (the northeast side in this case), in a region of strong vertical shear about a kilometer above the tropopause.

A picture of the actual cause of the incident is only possible with the DFDR information. Mesoscale winds and vertical velocities for Flight 125 were computed from a six-minute segment of flight data which culminated in the large altitude gain during the turbulence encounter, as described earlier. In this case, ATC radar fixes were not available, so integrations of INS data were initialized with position information from the pilot's log. Figures 3 and 4 show, respectively, a perspective diagram of the aircraft track over the smoothed terrain of southern Greenland and a vertical cross section of vertical velocity along the aircraft path. In Fig. 3, the region of available aircraft data falls between the thin vertical lines on either end of the bold portion of the aircraft track. Elsewhere, track and altitude are estimated from the pilot's log. The vertical velocities were first determined as described in section 2. Subsequently, a bias was removed from the derived vertical velocities by subtracting the mean value for the six-minute segment.

A mesoscale, wavelike variation clearly dominates the vertical motion in Fig. 4 near the location of the

turbulence occurrence (wavelength about 22 km). This pattern strongly suggests that the aircraft traversed the trough of a mountain lee wave over the western slopes of the Greenland icecap. Although no nearby upwind soundings were available for analysis within 12 hours of the incident, a careful reexamination of the available large-scale weather map analyses showed further evidence of the presence of mountain waves. For example, at the surface, a strong cross-mountain pressure gradient was present with the lowest pressures on the west side of Greenland; the easterly wind component at 500 mb increased from about 10 m s^{-1} at 1200 UTC on 22 January to nearly 20 m s^{-1} at 0000 UTC on 23 January. It is well known that these features are strong indicators of the presence of lee waves (e.g., see Nicholls 1973). At Narssarssuaq (the coastal station indicated in Fig. 3), at 1500 and 1800 UTC, surface winds were easterly at 10–15 m s^{-1}. This may be interpreted as a downslope wind condition, i.e., further circumstantial evidence of a local mountain wave effect.

A possible link between the mountain wave conditions and the surface winds described above is revealed by the horizontal wind field deduced from the DFDR data (Fig. 5). The rapid decrease of flight level windspeed to the point of the largest vertical motions suggests the presence of a critical level induced by the overturning of large amplitude mountain waves in the lower stratosphere. This feature is an important component of Clark and Peltier's (1977) explanation of strong downslope windstorms.

It is apparent from the additional mesoscale evidence provided here that the turbulence incident over southern Greenland on 22 January 1985 was likely due to mountain lee wave activity. The occurrence of mesoscale mountain wave phenomena in that area is not unusual (e.g., see Shapiro 1985; Scorer 1988). Furthermore, in 1985, there were at least two other cases of severe turbulence experienced by westbound commercial airliners over southern Greenland under synoptic conditions very similar to the present case (i.e., on 6 February 1985 and 25 November 1985).

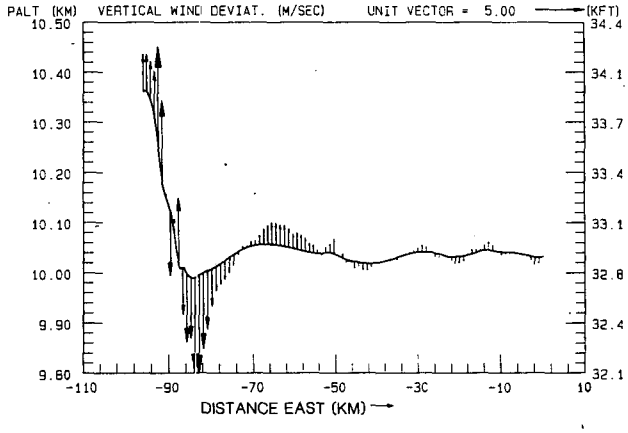

FIG. 4. Cross section along the aircraft track with derived vertical velocities superimposed at approximately 0.4-min intervals. The horizontal scale is labeled in distance relative to the beginning of the DFDR data segment. The right side of the diagram is the east end of the track. For comparison, a reference vector is shown in the upper right-hand corner of the diagram.

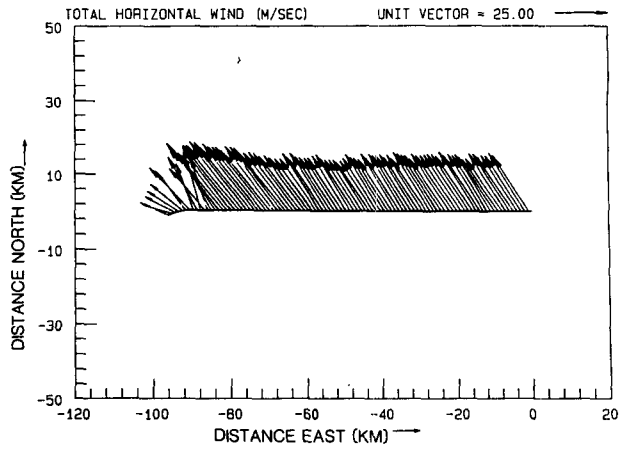

FIG. 5. Map showing aircraft track with derived wind vectors superimposed at 0.4-min intervals. Coordinates are relative to the beginning of the DFDR data segment with east on the right, and north at the top of the diagram. For comparison, a reference wind vector (m s^{-1}) is shown in the upper right-hand corner of the diagram.

4. Summary

The increasing availability of DFDR data from commercial aircraft is providing the scientific community with the opportunity for access to invaluable mesoscale information for the investigation of CAT and other small-scale meteorological phenomena. The processing of the DFDR data at NASA-Ames has been described and an example of the use of such information has been provided for a case of severe turbulence in mountain waves over southern Greenland.

Acknowledgments. The authors extend their thanks to Pan American Airlines for providing the flight data. Mr. Jack Molodonof and Mr. Vafa Kordestani provided capable programming assistance and Ms. Donna Hurth provided clerical expertise in the preparation of the manuscript. The research was supported under NASA Contract NCC 2-315.

REFERENCES

Bach, R. E., Jr., and E. K. Parks, 1987: Angle-of-attack estimation for analysis of windshear encounters. *J. Aircraft*, **24**, 789–792.
——, and R. C. Wingrove, 1989: The analysis of windshear from airline flight data. *J. Aircraft*, **26**, 103–109.
Clark, T. L., and W. R. Peltier, 1977: On the evolution and stability of finite amplitude mountain waves. *J. Atmos. Sci.*, **34**, 1715–1730.
Colson, D., 1963: Analysis of clear air turbulence for March 1962. *Mon. Wea. Rev.*, **91**, 73–82.

Dutton, J. A., 1969: An energy budget for a layer of stratosphere CAT. *Radio Sci.*, **4,** 1137–1142.

Ellrod, G., 1985: Indicators of high altitude, non-convective turbulence observed in satellite images. Preprints, *Conf. on the Aviation Weather System,* Montreal, Amer. Meteor. Soc., 277–284

Endlich, R. M., and R. L. Mancuso, 1965: On the analysis of clear air turbulence by use of radiosonde data. *Mon. Wea. Rev.*, **93,** 47–58.

Forrester, D. A., 1986: Transatlantic flight incident. *Meteor. Mag.*, **115,** 50–53.

Gysel, P., and H. Richner, 1986: Vertical air motion and turbulence parameters from commercial aircraft in scientific results of the Alpine Experiment (ALPEX). GARP Publ. Ser. No. 27, WMO/TD-NO. 108, 95–106.

Keller, J., 1986: Update on the SCATR Index: Validation at PROFS. AIAA 24th Aerospace Sciences Meeting. Paper AIAA-86-0256, Amer. Inst. Aeronaut. Astronaut, 4 pp.

Lenschow, D. H., 1986: Aircraft measurements in the boundary layer. *Probing the Atmospheric Boundary Layer,* Amer. Meteor. Soc., 269 pp.

Lester, P. F., and R. E. Bach, Jr., 1986: An extreme clear air turbulence incident associated with a strong downslope windstorm. AIAA 24 Aerospace Sciences Meeting, Reno, Paper AIAA-86-0329, Amer. Inst. Aeronaut. Astronaut, 7 pp.

Lilly, D. K., 1978: A severe downslope windstorm and aircraft turbulence event induced by a mountain wave. *J. Atmos. Sci.*, **35,** 59–77.

——, and E. L. Petersen, 1983: Aircraft measurements of atmospheric kinetic energy spectra. *Tellus,* **35A,** 379–382.

Nastrom, G. D., and K. S. Gage, 1983: A first look at wavenumber spectra from GASP data. *Tellus,* **35A,** 383–388.

Nicholls, J. M., 1973: The airflow over mountains: Research 1958–1972. WMO Tech. Note No. 127, 73 pp.

Parks, E. K., R. C. Wingrove, R. E. Bach, Jr. and R. S. Mehta, 1985: Identification of vortex-induced clear-air turbulence using airline flight records. *J. Aircraft,* **22,** 124–129.

Scorer, R. S., 1988: Sunny Greenland. *Quart. J. Roy. Meteor. Soc.*, **114,** 3–29.

Shapiro, M. A., 1985: Dropwind soundings of an Icelandic low and a Greenland mountain lee wave. *Mon. Wea. Rev.*, **113,** 680–683.